Engineering Applications of Artificial Intelligence 119 (2023) 105701

Contents lists available at ScienceDirect

Engineering Applications of Artificial Intelligence

journal homepage: www.elsevier.com/locate/engappai

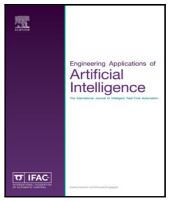

Permutation Jensen–Shannon divergence for Random Permutation Set

Luyuan Chen [a], Yong Deng [a,b,c,d,*], Kang Hao Cheong [e,**]

[a] Institute of Fundamental and Frontier Sciences, University of Electronic Science and Technology of China, Chengdu, China
[b] School of Education, Shaanxi Normal University, Xi'an, China
[c] School of Knowledge Science, Japan Advanced Institute of Science and Technology, Nomi, Ishikawa 923-1211, Japan
[d] Department of Management, Technology, and Economics, ETH Zurich, Zurich, Switzerland
[e] Science, Mathematics and Technology Cluster, Singapore University of Technology and Design, S487372, Singapore

ARTICLE INFO

Keywords:
Divergence measure
Jensen–Shannon divergence
Random permutation set
Evidence theory
Data fusion
Threat assessment

ABSTRACT

Random Permutation Set (RPS) considers the permutation of elements for a certain set, which is an efficient tool for dealing with uncertainty with ordered information. An important feature of RPS theory is that in the fusion rule of RPS sources, the fusion order has a great impact on fusion results. However, how to determine the fusion order has not yet been discussed. To address this problem, this paper first proposes Permutation Jensen–Shannon (PJS) divergence for measuring the distance between two RPSs. Based on PJS divergence, a new Reliability Assessment algorithm, named RAPJS, is then presented for determining the fusion order of RPSs. The proposed PJS divergence satisfies the properties of non–degeneracy, boundary, and symmetry, and has desirable compatibility with Belief Jensen–Shannon divergence and Jensen–Shannon divergence under certain conditions. The presented RAPJS makes use of the divergence information to calculate the reliability degree of RPS sources, the RPS with a higher reliability is fused first. Experiment results in threat assessment reveal that the presented RAPJS algorithm can determine the fusion order reasonably and effectively. The assessment results using the proposed RAPJS algorithm has the highest target recognition rate compared to other results under different fusion orders.

1. Introduction

The management and combination of uncertain information is a problem of importance and has attracted immense interests in engineering applications of artificial intelligence (Tang et al., 2020; Pan et al., 2020; Agushaka et al., 2022b). A wide variety of theories has been developed for the processing of uncertainty, for instance, probability theory (Lee, 1980), fuzzy sets (Zadeh, 1996), intuitionistic fuzzy sets (Atanassov, 1999; Song et al., 2018), evidence theory (Yang and Han, 2016; Chen and Deng, 2022b), and Random permutation set (RPS) (Deng, 2022), which have been applied in many applications, for instance, information fusion (Lai et al., 2020; Deng and Wang, 2021), risk assessment (Gao et al., 2022b; Rani et al., 2019; Chen et al., 2021b), complexity networks (Wen and Cheong, 2021; Wu et al., 2022d), target recognition (Wen et al., 2021; Zhang et al., 2022), classification and classifier (Xiao and Pedrycz, 2022; Liu et al., 2020), time analysis (Cui et al., 2022; Song and Xiao, 2022) and decision making (Chen et al., 2021a; Xu et al., 2021; Abualigah et al., 2021b).

By considering the concept of order, Deng extended evidence theory and presented random permutation set (RPS) theory (Deng, 2022). By combining orderable sets (Zhang and Deng, 2021) and permutation function (Bordenave and Collins, 2019), RPS is efficient in representing ordered information by permutation event space (PES) and permutation mass function (PMF), as well as combining several RPS sources by Permutation orthogonal sum (POS). RPS has been applied in decision making (Deng, 2022), uncertainty measure (Chen and Deng, 2022a; Deng and Deng, 2022) and risk assessment (Deng, 2022).

POS provides the fusion rule for different RPS sources, which includes two types of rule: left orthogonal sum (LOS) and right orthogonal sum. An important feature of POS is that different fusion orders will produce different fusion results (Deng, 2022). In general, the RPS source with a higher reliability (or weight) is combined first, which has a greater impact on final fusion results (Deng, 2022). For example, regarding two permutation events (A, B) and (B, A), if (A, B) is fused first and (B, A) is second, the fusion results by LOS is (A, B). While if (B, A) is fused first and (A, B) is second, the fusion results by LOS is (B, A). The fusion order has a significant effect on fusion performance by POS. Therefore, how to determine the order of RPSs in fusion process is an important problem, yet remains unsolved.

As an efficient tool for comparing the description of objects, divergence measure has been successfully applied in many fields of artificial intelligence (Fan et al., 2021; Joshi and Kumar, 2019a; Wu

* Corresponding author at: Institute of Fundamental and Frontier Sciences, University of Electronic Science and Technology of China, Chengdu, China.
** Corresponding author at: Science, Mathematics and Technology Cluster, Singapore University of Technology and Design, S487372, Singapore.
E-mail addresses: dengentropy@uestc.edu.cn (Y. Deng), kanghao_cheong@sutd.edu.sg (K.H. Cheong).

https://doi.org/10.1016/j.engappai.2022.105701
Received 8 September 2022; Received in revised form 29 November 2022; Accepted 29 November 2022
Available online 19 December 2022

Table 1
Symbol appointment.

Parameter	Description
Γ	A fixed set with N elements
$m(\cdot)$	A mass function
$PES(\Gamma)$	Permutation event space of Γ
$\mathscr{M}(\cdot)$	Permutation mass function
$P(N,i)$	The i-permutation of N
P, Q	Probability distribution
D_{JS}	Jensen–Shannon divergence value
D_{BJS}	Belief Jensen–Shannon divergence value
D_{PJS}	Permutation Jensen–Shannon divergence value
$RTD(\cdot)$	The relative threat degree for a threat event
FTA	The final threat assessment
$\widetilde{D_{PJS}}(\cdot)$	The average distance of RPS
$\widetilde{Sup_{PJS}}(\cdot)$	The support degree of RPS
$W(\cdot)$	The reliability degree of RPS

et al., 2022a). Jensen–Shannon (JS) divergence is one of the most well-known divergence measures, which has been pivotal in measuring the discrimination of two probability distributions (Lin, 1991). JS divergence has some desirable properties including symmetry, boundary and triangle inequality. Due to the advantage in measuring discrepancy, JS divergence has been extended to other theories including fuzzy sets (Mishra et al., 2020a; Li et al., 2014), intuitionistic fuzzy sets (Joshi and Kumar, 2019b; Mishra et al., 2020b), T-spherical fuzzy sets (Wu et al., 2019) and evidence theory (Xiao, 2020; Wang et al., 2021). For example, in evidence theory, Xiao proposes a belief Jensen–Shannon divergence (BJS) measure for quantifying the discrepancy between mass functions (Xiao, 2019). Gao et al. define a generalized divergence based on information volume and apply to iris classification and fault diagnosis (Gao et al., 2022a). Pan et al. propose an enhanced JS divergence considering both the internal and external difference between mass functions (Pan et al., 2022). However, the divergence measure between two PMFs in RPS has not yet been discussed.

Aimed at addressing the issue of the fusion order in POS, Permutation Jensen–Shannon (PJS) divergence is first proposed for measuring the distance between two RPSs. Based on PJS divergence, a new Reliability Assessment algorithm (RAPJS) is then presented for determining the fusion order of RPSs. The proposed PJS divergence satisfies the properties of non–degeneracy, boundary, and symmetry, and has desirable compatibility with BJS divergence and JS divergence under certain conditions. Based on PJS divergence, the presented RAPJS considers the similarity between RPSs, the RPS which has a larger similarity (or support) has a higher reliability and is fused first, thus the order of RPSs in fusion process can be determined. Experiment results in threat assessment reveal that the RAPJS algorithm can determine the fusion order reasonably and effectively. The threat assessment result using the proposed RAPJS algorithm has the highest recognition rate compared to results under other fusion orders.

The rest of this paper is as follows. Section 2 introduces some related background knowledge. Section 3 proposes the PJS divergence for RPS. Section 4 uses several numerical examples to illustrate the presented PJS measure. Section 5 puts forward the RAPJS algorithm and demonstrates its application in threat assessment. Section 6 concludes the paper.

2. Preliminaries

Some preliminaries related to the paper are briefly reviewed in this section. Notations adopted in this article are summarized in Table 1.

2.1. Evidence theory

The era of big data has brought massive amounts of data (Yuan et al., 2020; Oyelade et al., 2022; Agushaka et al., 2022a). Uncertain information also comes with increasing and has always been in our daily life (Deng, 2020; Xiao, 2022; Wu et al., 2022b). Evidence theory, being a significant theory for uncertainty reasoning, is a crucial and beneficial tool that has been widely applied in information fusion (Zhao et al., 2022; Zhou et al., 2022). The basic concept of mass function is introduced.

Definition 2.1 (*Mass Function*)**.** Given a fixed set of N elements $\Gamma = \{\tau_1, \tau_2, \ldots, \tau_N\}$, a mass function is a mapping from 2^Γ to [0, 1], formally defined by (Dempster, 1967; Shafer, 1976)

$$m : 2^\Gamma \to [0,1] \tag{1}$$

constrained by

$$\sum_{A\in 2^\Gamma} m(A) = 1, \quad m(\varnothing) = 0 \tag{2}$$

where 2^Γ is the power set of Γ, $\varnothing$ means the empty set.

2.2. Random permutation set

As a novel technique to manage with uncertainty with ordered information, RPS has been proposed which considers the permutation of elements in a certain set (Deng, 2022). Some basic concepts of RPS are introduced.

Definition 2.2 (*Permutation Event Space (PES)*)**.** Given a fixed set of N elements $\Gamma = \{\tau_1, \tau_2, \ldots, \tau_N\}$, PES is a set containing all permutations in Γ, defined by (Deng, 2022)

$$\begin{aligned} PES(\Gamma) &= \{ A_{ij} \} \qquad (3)\\ &= \{ \varnothing, (\tau_1), (\tau_2), \ldots, (\tau_N), (\tau_1,\tau_2), (\tau_2,\tau_1), \ldots, (\tau_{N-1},\tau_N), \\ &\quad (\tau_N,\tau_{N-1}), \ldots, (\tau_1,\tau_2,\ldots,\tau_N), \ldots, (\tau_N,\tau_{N-1},\ldots,\tau_1) \} \qquad (4) \end{aligned}$$

where $i \in [0, N], j \in [1, P(N,i)]$. $P(N,i) = \frac{N!}{(N-i)!}$, which is the i-permutation of N. The element A_{ij} in PES is called a permutation event. The cardinality of $PES(\Gamma)$ is $\Delta = \sum_{i=0}^{N} P(N,i)$.

Definition 2.3 (*Random Permutation Set (RPS)*)**.** Given a fixed set of N elements $\Gamma = \{\tau_1, \tau_2, \ldots, \tau_N\}$, RPS is a set of pairs defined by (Deng, 2022):

$$RPS(\Gamma) = \{\langle A, \mathscr{M}(A)\rangle \mid A \in PES(\Gamma)\} \tag{5}$$

where $\mathscr{M}$ is called permutation mass function (PMF), described as:

$$\mathscr{M} : PES(\Gamma) \to [0,1] \tag{6}$$

satisfying

$$\mathscr{M}(\varnothing) = 0, \quad \sum_{A\in PES(\Gamma)} \mathscr{M}(A) = 1 \tag{7}$$

Definition 2.4 (*Left Orthogonal Sum (LOS)*)**.** Given two RPSs defined on Γ: $RPS_1 = \{\langle A_1, \mathscr{M}_1(A_1)\rangle\}$ and $RPS_2 = \{\langle A_2, \mathscr{M}_2(A_2)\rangle\}$, the left orthogonal sum (LOS), represented by $\mathscr{M}^L = RPS_1 \overleftarrow{\oplus} RPS_2$, is defined by (Deng, 2022)

$$\mathscr{M}^L(A) = \begin{cases} \frac{1}{1-\overleftarrow{K}} \sum\limits_{A_1 \overleftarrow{\cap} A_2 = A} \mathscr{M}_1(A_1)\mathscr{M}_2(A_2), & \mathrm{A} \neq \varnothing \\ 0, & \mathrm{A} = \varnothing \end{cases} \tag{8}$$

where $A_1, A_2 \in PES(\Gamma)$, $A_1 \overleftarrow{\cap} A_2 = A_1 \setminus\setminus \bigcup_{\tau\in A_1, \tau\notin A_2} \{\tau\}$. Note for any two sets B and C, $B\setminus\setminus C$ denotes removing C from B under the permutation of elements in B. $\overleftarrow{K}$ is defined as

$$\overleftarrow{K} = \sum_{A_1 \overleftarrow{\cap} A_2 = \varnothing} \mathscr{M}_1(A_1)\mathscr{M}_2(A_2) \tag{9}$$

Some important properties about RPS are discussed in Deng (2022).

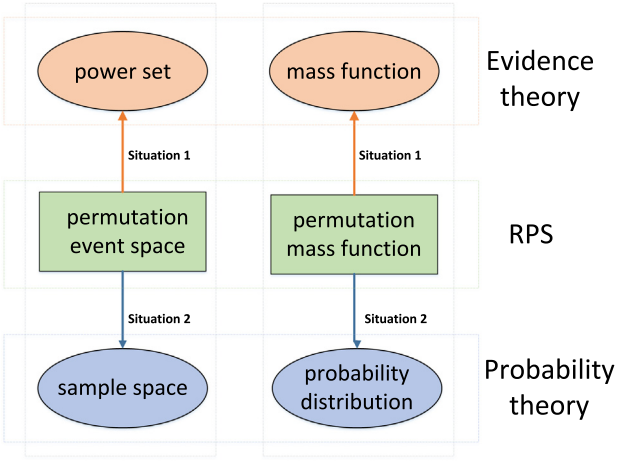

Fig. 1. The relationships between RPS, evidence theory and probability theory.

Remark 2.1. When not considering the permutation of elements in PES, the PES of RPS is the same as power set, the PMF of PFS is the same as mass function in evidence theory.

Remark 2.2. When each permutation event is singleton, the PES of RPS degenerates into sample space, the PMF of PFS degenerates into probability distribution.

Specifically, Fig. 1 shows the relationship between RPS, evidence theory and probability theory.

2.3. Jensen–Shannon divergence

Divergence is an efficient mathematical tool for measuring the difference between two distributions, and is widely used in many applications such as pattern recognition (Wu et al., 2022c; Chen and Cai, 2022; Wu et al., 2021), decision making (Song et al., 2019; Kharazmi and Balakrishnan, 2021), fault diagnosis (Joshi and Kumar, 2019c; Zhao et al., 2021), supply chain management (Jiao et al., 2018) and optimization (Abualigah et al., 2021a; Ezugwu et al., 2022; Abualigah et al., 2022). Various kinds of divergence measures have been proposed, such as Kullback–Leibler divergence (Moreno et al., 2003; Gao et al., 2019), β divergence (Carabias-Orti et al., 2013), $\alpha-\beta$ divergence (Shang et al., 2021), χ divergence (Kharazmi et al., 2022) and J-divergence (Zhang et al., 2020). As a popular method for measuring the difference between two probability distributions, a brief introduction of Jensen–Shannon (JS) divergence is as follows.

Definition 2.5. For two probability distributions $P=\{p_1,p_2,\ldots,p_n\}$ and $Q=\{q_1,q_2,\ldots,q_n\}$ defined on a discrete random variable, the Jensen–Shannon (JS) divergence between P and Q is defined by (Lin, 1991)

$$D_{JS}(P,Q)=\frac{1}{2}\left[H\left(P,\frac{P+Q}{2}\right)+H\left(Q,\frac{P+Q}{2}\right)\right] \tag{10}$$

where $H(P,Q)$ is Kullback–Leibler divergence calculated by $H(P,Q)=\sum_i p_i\ log_2\frac{p_i}{q_i}$.

As a strict distance measure, JS divergence satisfies the following properties:

- Symmetry: $D_{JS}(P,Q)=D_{JS}(Q,P)$
- Boundary: $D_{JS}(P,Q)\in[0,1]$
- Triangle inequality: $\sqrt{D_{JS}(P,Q)}+\sqrt{D_{JS}(P,T)}\geqslant\sqrt{D_{JS}(Q,T)}$

2.4. Belief Jensen–Shannon divergence

For measuring the difference between two mass functions, Xiao extended JS divergence to Belief Jensen–Shannon (BJS) divergence.

Definition 2.6. Giver two mass functions m_1 and m_2 defined on a set Γ, the belief Jensen–Shannon divergence between m_1 and m_2 is defined by (Xiao, 2019)

$$D_{BJS}(m_1,m_2)=\frac{1}{2}\left[H\left(m_1,\frac{m_1+m_2}{2}\right)+H\left(m_2,\frac{m_1+m_2}{2}\right)\right] \tag{11}$$

where $H(m_1,m_2)=\sum_{A_i\in2^\Gamma}m_1(A_i)\ log_2\frac{m_1(A_i)}{m_2(A_i)}$.

Similarly, BJS divergence satisfies the properties of symmetry, boundary and triangle inequality (Xiao, 2019). When mass function turns into probability, BJS degenerates into JS.

3. Permutation Jensen–Shannon divergence for random permutation set

In Random permutation set, the discrepancy measure among permutation mass functions is still an open problem. By extending the classical JS divergence into Random permutation set, a novel divergence measure named Permutation Jensen–Shannon (PJS) divergence is introduced as below.

Definition 3.1. Given a fixed set Γ with N elements $\Gamma=\{\tau_1,\tau_2,\ldots,\tau_N\}$, $RPS_1=\{\langle A_{ij},\mathscr{M}_1(A_{ij})\rangle\}$ and $RPS_2=\{\langle A_{ij},\mathscr{M}_2(A_{ij})\rangle\}$, the Permutation Jensen–Shannon divergence measure between RPS_1 and RPS_2, denoted by D_{PJS}, is defined as

$$\begin{aligned}D_{PJS}(RPS_1,RPS_2)=\frac{1}{2}&\left[H\left(RPS_1,\frac{RPS_1+RPS_2}{2}\right)\right.\\&\left.+H\left(RPS_2,\frac{RPS_1+RPS_2}{2}\right)\right]\end{aligned} \tag{12}$$

where $H(RPS_1,RPS_2)$ is calculated by

$$H(RPS_1,RPS_2)=\sum_{A_{ij}\in PES(\Gamma)}\mathscr{M}_1(A_{ij})\log\left(\frac{\mathscr{M}_1(A_{ij})}{\mathscr{M}_2(A_{ij})}\right) \tag{13}$$

Therefore, Eq. (12) can be rewritten as

$$\begin{aligned}&D_{PJS}(RPS_1,RPS_2)\\&=\frac{1}{2}\left[\begin{array}{l}\sum_{A_{ij}\in PES(\Gamma)}\mathscr{M}_1(A_{ij})\log\left(\frac{2.\mathscr{M}_1(A_{ij})}{\mathscr{M}_1(A_{ij})+\mathscr{M}_2(A_{ij})}\right)\\+\sum_{A_{ij}\in PES(\Gamma)}\mathscr{M}_2(A_{ij})\log\left(\frac{2.\mathscr{M}_2(A_{ij})}{\mathscr{M}_1(A_{ij})+\mathscr{M}_2(A_{ij})}\right)\end{array}\right]\end{aligned} \tag{14}$$

where $i\in[0,N],j\in[1,P(N,i)]$. $P(N,i)=\frac{N!}{(N-i)!}$, which is the i-permutation of N.

Obviously, the proposed PJS divergence has the same form with the classic JS divergence. However, the presented PJS divergence substitutes probability distribution with permutation mass functions, which thus can model the difference for RPS. The property of the proposed PJS can be directly inferred as follows:

- Symmetry: $D_{PJS}(RPS_1,RPS_2)=D_{PJS}(RPS_2,RPS_1)$
- Boundary: $0\leqslant D_{PJS}(RPS_1,RPS_2)\leqslant 1$
- Triangle inequality: $\sqrt{D_{PJS}(RPS_1,RPS_2)}+\sqrt{D_{PJS}(RPS_1,RPS_3)}\geqslant\sqrt{D_{PJS}(RPS_2,RPS_3)}$

In addition, some remarks on JS, BJS and the presented PJS divergence measures are discussed.

Remark 3.1. The proposed PJS divergence degenerates to BJS divergence when the order in permutation events is not considered, i.e., when PMF turns into mass function.

Remark 3.2. The proposed PJS divergence degenerates to JS divergence when the elements in permutation events are single, i.e., when PMF turns into probability.

4. Numerical examples and discussion

In this section, some numerical examples are shown to illustrate the presented PJS divergence for RPS.

Example 4.1. Given two RPSs RPS_1 and RPS_2 in the fixed set $\Gamma = \{\tau_1, \tau_2, \tau_3\}$, and the two RPSs are given as follows:

$$RPS_1 = \{\langle(\tau_1), 0.4\rangle, \langle(\tau_2, \tau_3), 0.1\rangle, \langle(\tau_1, \tau_2, \tau_3), 0.15\rangle, \langle(\tau_2, \tau_3, \tau_1), 0.35\rangle\}$$
$$RPS_2 = \{\langle(\tau_1), 0.4\rangle, \langle(\tau_2, \tau_3), 0.1\rangle, \langle(\tau_1, \tau_2, \tau_3), 0.15\rangle, \langle(\tau_2, \tau_3, \tau_1), 0.35\rangle\}$$

As shown in Example 4.1, it can be found that RPS_1 has the same PMFs as RPS_2, where $\mathscr{M}_1(\tau_1) = \mathscr{M}_2(\tau_1) = 0.4$, $\mathscr{M}_1(\tau_2, \tau_3) = \mathscr{M}_2(\tau_2, \tau_3) = 0.1$, $\mathscr{M}_1(\tau_1, \tau_2, \tau_3) = \mathscr{M}_2(\tau_1, \tau_2, \tau_3) = 0.15$ and $\mathscr{M}_1(\tau_2, \tau_3, \tau_1) = \mathscr{M}_2(\tau_2, \tau_3, \tau_1) = 0.35$. The specific calculation process of PJS divergence $D_{PJS}(RPS_1, RPS_2)$ is shown as below:

$$\begin{aligned} D_{PJS}(RPS_1, RPS_2) =& \frac{1}{2} \times 0.4 \times log(\frac{2 \times 0.4}{0.4 + 0.4}) + \frac{1}{2} \times 0.4 \times log(\frac{2 \times 0.4}{0.4 + 0.4}) \\ &+ \frac{1}{2} \times 0.1 \times log(\frac{2 \times 0.1}{0.1 + 0.1}) + \frac{1}{2} \times 0.1 \times log(\frac{2 \times 0.1}{0.1 + 0.1}) \\ &+ \frac{1}{2} \times 0.15 \times log(\frac{2 \times 0.15}{0.15 + 0.15}) + \frac{1}{2} \times 0.15 \\ &\times log(\frac{2 \times 0.15}{0.15 + 0.15}) \\ &+ \frac{1}{2} \times 0.35 \times log(\frac{2 \times 0.35}{0.35 + 0.35}) + \frac{1}{2} \times 0.35 \\ &\times log(\frac{2 \times 0.35}{0.35 + 0.35}) \\ =& 0 \end{aligned}$$

This example shows that when RPS_1 has the same PMFs as RPS_2, the proposed PJS divergence between RPS_1 and RPS_2 equals to 0 which accords with an intuitionistic result.

Example 4.2. Given two RPSs RPS_1 and RPS_2 in the fixed set $\Gamma = \{\tau_1, \tau_2, \tau_3\}$, and the two RPSs are given as follows:

$$RPS_1 = \{\langle(\tau_1), 0.4\rangle, \langle(\tau_2, \tau_3), 0.2\rangle, \langle(\tau_1, \tau_2, \tau_3), 0.05\rangle, \langle(\tau_2, \tau_3, \tau_1), 0.35\rangle\}$$
$$RPS_2 = \{\langle(\tau_1), 0.5\rangle, \langle(\tau_2, \tau_3), 0.1\rangle, \langle(\tau_1, \tau_2, \tau_3), 0.15\rangle, \langle(\tau_2, \tau_3, \tau_1), 0.25\rangle\}$$

From Example 4.2, it can be seen that RPS_1 has different PMFs to RPS_2, for example, RPS_1 has a smaller chance value to support the event τ_1, where $\mathscr{M}_1(\tau_1) = 0.4$ and $\mathscr{M}_2(\tau_1) = 0.5$. The proposed PJS divergence $D_{PJS}(RPS_1, RPS_2)$ is calculated as follows:

$$\begin{aligned} D_{PJS}(RPS_1, RPS_2) =& \frac{1}{2} \times 0.4 \times log(\frac{2 \times 0.4}{0.4 + 0.5}) + \frac{1}{2} \times 0.5 \times log(\frac{2 \times 0.5}{0.5 + 0.4}) \\ &+ \frac{1}{2} \times 0.2 \times log(\frac{2 \times 0.2}{0.2 + 0.1}) + \frac{1}{2} \times 0.1 \times log(\frac{2 \times 0.1}{0.1 + 0.2}) \\ &+ \frac{1}{2} \times 0.05 \times log(\frac{2 \times 0.05}{0.05 + 0.15}) + \frac{1}{2} \times 0.15 \\ &\times log(\frac{2 \times 0.15}{0.15 + 0.05}) \\ &+ \frac{1}{2} \times 0.35 \times log(\frac{2 \times 0.35}{0.35 + 0.25}) + \frac{1}{2} \times 0.25 \\ &\times log(\frac{2 \times 0.25}{0.25 + 0.35}) \\ =& 0.0412 \end{aligned}$$

Similarly, the PJS divergence between RPS_1 and RPS_2 can be calculated as $D_{PJS}(RPS_2, RPS_1) = 0.0412$.

From the above results, it can be seen that the PJS divergence between RPS_1 and RPS_2 $D_{PJS}(RPS_1, RPS_2)$ is the same as the divergence measure between RPS_2 and RPS_1 $D_{PJS}(RPS_2, RPS_1)$. In a word, the symmetric property of PJS divergence is verified in this example.

Example 4.3. Followed by Example 4.2, if the order of elements in permutation events is not considered, like that (τ_1, τ_2, τ_3) and (τ_2, τ_3, τ_1) are equal sets, the two RPSs are changed as

$$RPS_1 = \{\langle(\tau_1), 0.4\rangle, \langle(\tau_2, \tau_3), 0.2\rangle, \langle(\tau_1, \tau_2, \tau_3), 0.4\rangle\}$$
$$RPS_2 = \{\langle(\tau_1), 0.5\rangle, \langle(\tau_2, \tau_3), 0.1\rangle, \langle(\tau_1, \tau_2, \tau_3), 0.4\rangle\}$$

Based on Remark 2.1, the two RPSs can be regarded as two mass functions in evidence theory:

$$m_1(\tau_1) = 0.4, m_1(\tau_2, \tau_3) = 0.2, m_1(\tau_1, \tau_2, \tau_3) = 0.4$$
$$m_2(\tau_1) = 0.5, m_2(\tau_2, \tau_3) = 0.1, m_2(\tau_1, \tau_2, \tau_3) = 0.4$$

According to Eq. (12), the associated PJS divergence between RPS_1 and RPS_2 is computed with the result $D_{PJS}(RPS_1, RPS_2) = 0.0163$. In addition, based on Eq. (11), the associated BJS divergence between m_1 and m_2 is calculated with the result $D_{BJS}(m_1, m_2) = 0.0163$. Obviously, $D_{PJS}(RPS_1, RPS_2) = D_{BJS}(m_1, m_2)$. Consequently, as stated in Remark 3.1, if the order in permutation events is not considered, the proposed PJS divergence degenerates into BJS divergence.

Example 4.4. Followed by Example 4.3, let $X = \{\tau_1\}, Y = \{\tau_2, \tau_3\}, Z = \{\tau_1, \tau_2, \tau_3\}$. Under the new fixed set $\Omega = \{X, Y, Z\}$, each permutation event just contains one element, the two RPSs turn into

$$RPS_1 = \{\langle(X), 0.4\rangle, \langle(Y), 0.2\rangle, \langle(Z), 0.4\rangle\}$$
$$RPS_2 = \{\langle(X), 0.5\rangle, \langle(Y), 0.1\rangle, \langle(Z), 0.4\rangle\}$$

Based on Remark 2.2, the two RPSs can be regarded as two probability distributions:

$$p_1(X) = 0.4, p_1(Y) = 0.2, p_1(Z) = 0.4$$
$$p_2(X) = 0.5, p_2(Y) = 0.1, p_2(Z) = 0.4$$

According to Eq. (12), the associated PJS divergence measure between RPS_1 and RPS_2 is given with the result $D_{PJS}(RPS_1, RPS_2) = 0.0163$. In addition, based on Eq. (10), the associated JS divergence between p_1 and p_2 is calculated with the result $D_{JS}(p_1, p_2) = 0.0163$. Obviously, $D_{PJS}(RPS_1, RPS_2) = D_{JS}(p_1, p_2)$. Consequently, as stated in Remark 3.2, if all of permutation events are single elements, the proposed PJS divergence degenerates into the classic JS divergence.

Example 4.5. Given three RPSs RPS_1, RPS_2 and RPS_3 defined in the fixed set $\Gamma = \{\tau_1, \tau_2\}$, and the three RPSs are given as follows:

$$RPS_1 = \{\langle(\tau_1), 0.3\rangle, \langle(\tau_2), 0.2\rangle, \langle(\tau_1, \tau_2), 0.5\rangle\}$$
$$RPS_2 = \{\langle(\tau_1), 0.2\rangle, \langle(\tau_2), 0.6\rangle, \langle(\tau_1, \tau_2), 0.2\rangle\}$$
$$RPS_3 = \{\langle(\tau_1), 0.5\rangle, \langle(\tau_1, \tau_2), 0.3\rangle, \langle(\tau_2, \tau_1), 0.2\rangle\}$$

As shown in Example 4.5, we can see that both PMFs in RPS_1 and RPS_2 are assigned on single elements, i.e., (τ_1) and (τ_2), and multiple elements, i.e., (τ_1, τ_2), while PMFs in RPS_3 are also distributed to multiple elements with different orders, i.e., (τ_1, τ_2) and (τ_2, τ_1). Divergence measures between different RPSs and the corresponding square root values are calculated, just shown as below:

$$D_{PJS}(RPS_1, RPS_2) = 0.1307; \ \sqrt{D_{PJS}(RPS_1, RPS_2)} = 0.3615$$
$$D_{PJS}(RPS_1, RPS_3) = 0.2365; \ \sqrt{D_{PJS}(RPS_1, RPS_3)} = 0.4863$$
$$D_{PJS}(RPS_2, RPS_3) = 0.4552; \ \sqrt{D_{PJS}(RPS_2, RPS_3)} = 0.6747$$

It can be noticed that $\sqrt{D_{PJS}(RPS_1, RPS_2)} + \sqrt{D_{PJS}(RPS_1, RPS_3)} = 0.8477$, so that $\sqrt{D_{PJS}(RPS_1, RPS_2)} + \sqrt{D_{PJS}(RPS_1, RPS_3)} > \sqrt{D_{PJS}(RPS_2, RPS_3)}$, which satisfies the triangle inequality property of the proposed PJS divergence method.

Example 4.6. Given two RPSs RPS_1 and RPS_2 defined on the fixed set $\Gamma = \{\tau_1, \tau_2\}$, and the two RPSs are given as follows:

$$RPS_1 = \{\langle(\tau_1), \alpha\rangle, \langle(\tau_2), 0.02\rangle, \langle(\tau_1, \tau_2), 0.97 - \alpha\rangle, \langle(\tau_2, \tau_1), 0.01\rangle\}$$
$$RPS_2 = \{\langle(\tau_1), \beta\rangle, \langle(\tau_2), 0.02\rangle, \langle(\tau_1, \tau_2), 0.97 - \beta\rangle, \langle(\tau_2, \tau_1), 0.01\rangle\}$$

As shown in Example 4.6, both RPS_1 and RPS_2 contain all kinds of permutation events in PES (Γ), and the permutation mass function values are controlled by α and β respectively. As the parameters α and β change from 0 to 0.97, the variation of the proposed PJS divergence measure between RPS_1 and RPS_2 is depicted in Fig. 2.

Fig. 2 shows that PJS divergence values are always in the range of [0, 1] and are symmetric to the plane Y = X, which verifies the

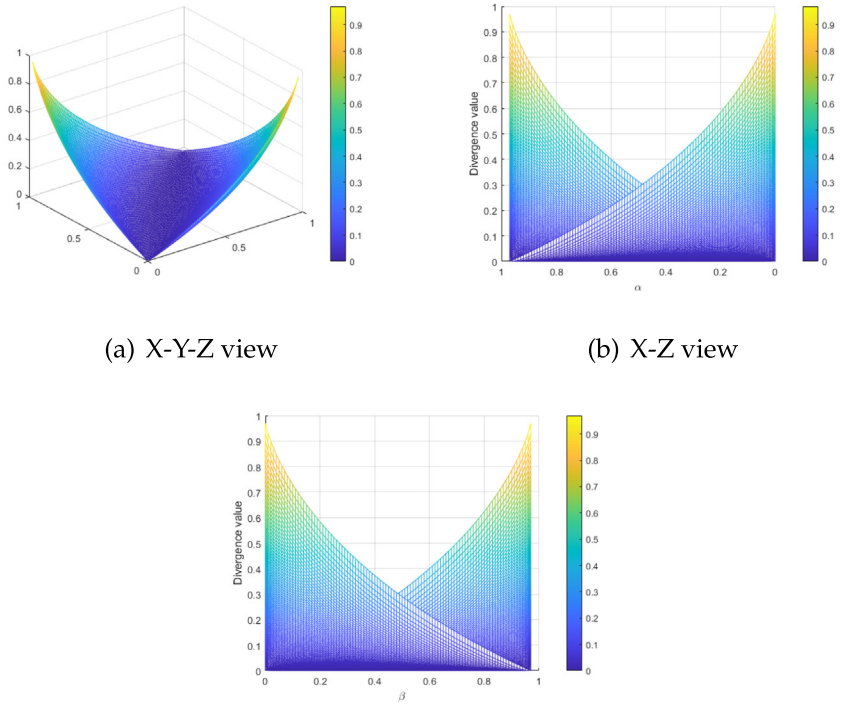

(a) X-Y-Z view (b) X-Z view

(c) Y-Z view

Fig. 2. The variation of PJS divergence values.

boundary and symmetric properties of PJS divergence. When $\alpha = \beta = 0$, RPS_1 is the same as RPS_2, $D_{PJS}(RPS_1, RPS_2)$ has the minimum value with 0. When $\alpha = 0, \beta = 0.97$ or $\alpha = 0.97$, $\beta = 0$, $D_{PJS}(RPS_1, RPS_2)$ reaches the maximum value. Correspondingly, as shown in Fig. 2(b) which is from the perspective of α, as α increases from 0 to 0.49, the maximum PJS value between RPS_1 and RPS_2 gradually decreases. As α increases from 0.49 to 0.97, the maximum PJS value between RPS_1 and RPS_2 gradually increases. Fig. 2(c) has the same curve rule from the perspective of β.

5. Application in threat assessment

The concept of order is ubiquitous in real world, for instance, the chronological order in time domain Yuan et al. (2022) and Qiang et al. (2022) and the behavior order in decision making (Chen and Deng, 2022c). Ordered information also plays a critical role in military operations (Deng, 2022). For example, in a scenario of enemy aircraft detection, it cannot fully access the threat based on the type and number of enemy aircraft, since different formations and orders of aircraft will produce distinct results. Therefore, it is necessary to model ordered information in enemy aircraft detection, where RPS is an alternative to address this problem.

Assume three types of aircraft (potential threatening targets) are considered represented by $\Gamma = \{A, B, C\}$. In the context of RPS, $PES(\Gamma)$ denotes all possible threat events. The cardinality of threat events denotes the corresponding type of threat events. PMF defined on $PES(\Gamma)$ represents the threat degree of threat events, and the order in permutation events denotes the threat ranking. For example, a report of $\langle (C, B, A), 0.65 \rangle$ means that the enemy may dispatch all three types of aircraft, among which C is the most threatening, B is the next, while the threat of A is the lowest. The occurrence chance of (C, B, A) is relatively high with 0.65. Given several reports from different radars, Deng has proposed a RPS-based data fusion (RPSDF) algorithm for fusing these reports to make a comprehensive assessment (Deng, 2022). The detailed procedures of RPSDF are shown in Algorithm 1.

Algorithm 1: The RPS-based data fusion algorithm (RPSDF) (Deng, 2022)

Input: The set of the type of aircraft: $\Gamma = \{\tau_1, \tau_2, \ldots, \tau_N\}$, Threat assessment reports represented by M RPSs.

Output: The predicted target for each type of threat event

1 Based on a specific order of RPSs, combine M RPSs based on LOS:

$$\mathscr{M}^L = RPS_1 \overline{\oplus} RPS_2 \overline{\oplus} \ldots \overline{\oplus} RPS_M \tag{15}$$

2 Compute the relative threat degree (RTD) for each threat event A_{ij}.

$$RTD(A_{ij}) = \frac{\mathscr{M}^L(A_{ij})}{\sum_{j=1}^{P(N,i)} \mathscr{M}^L(A_{ij})} \tag{16}$$

where $i \in [1, N]$, $j \in [1, P(N, i)]$

3 Determine the final threat assessment (FTA) for all types of threat events:

$$FTA_i = argmax_{1 \le j \le P(N,i)}[RTD(A_{ij})] \tag{17}$$

4 return FTA_i;

A critical step in the RPSDF algorithm is determining the fusion order of RPSs. Unfortunately, it just gives a hypothetical expert-based reliability ranking, which is invalid. To address this problem, a new Reliability Assessment algorithm based on the proposed PJS, referred to as RAPJS, is presented to determine the fusion order of RPSs. The RPS which has a higher reliability is combined first. The complete framework for threat assessment is shown in Fig. 3.

5.1. The proposed reliability assessment algorithm (RAPJS)

Given M RPSs defined on a fixed set Γ, the presented RAPJS algorithm is described as follows:

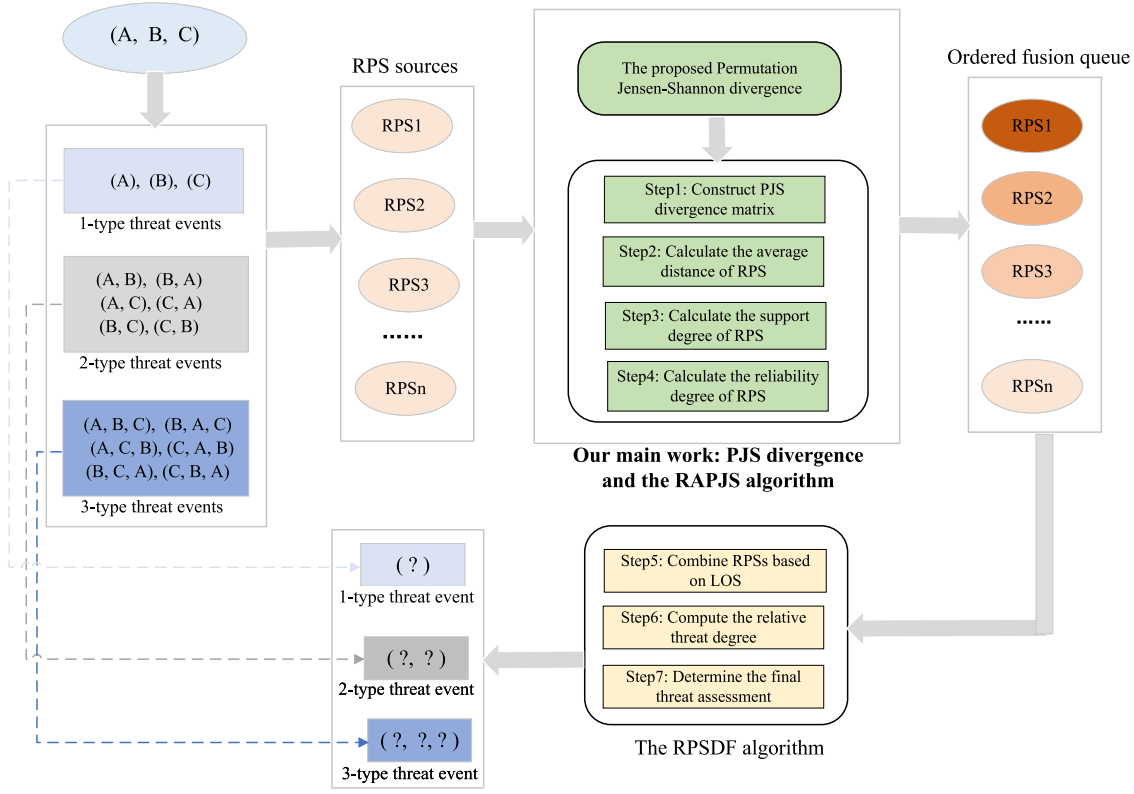

Fig. 3. The framework for threat assessment.

Step 5-1: By using the presented PJS divergence measure, the distance between different RPSs can be obtained. A PJS divergence measure matrix, i.e., a distance matrix, $DM = [D_{PJS}(RPS_i, RPS_j)]_{M\times M}$, $i, j \in [1, M]$, is constructed as follows:

$$DM = \begin{bmatrix} 0 & \cdots & D_{PJS}(RPS_1, RPS_i) & \cdots & D_{PJS}(RPS_1, RPS_M) \\ \vdots & \cdots & \vdots & \cdots & \vdots \\ D_{PJS}(RPS_i, RPS_1) & \cdots & 0 & \cdots & D_{PJS}(RPS_i, RPS_M) \\ \vdots & \cdots & \vdots & \cdots & \vdots \\ D_{PJS}(RPS_M, RPS_1) & \cdots & D_{PJS}(RPS_M, RPS_i) & \cdots & 0 \end{bmatrix} \tag{18}$$

Step 5-2: Calculate the average distance of RPS_i to other RPSs:

$$\widetilde{D_{PJS}(RPS_i)} = \frac{\sum_{j=1}^{M} D_{PJS}(RPS_i, RPS_j)}{M-1} \tag{19}$$

Step 5-3: Calculate the support degree of RPS_i:

$$Sup(RPS_i) = \frac{1}{\widetilde{D_{PJS}(RPS_i)}} \tag{20}$$

Step 5-4: The reliability degree of RPS_i is defined as:

$$W(RPS_i) = \frac{Sup(RPS_i)}{\sum_{j=1}^{M} Sup(RPS_j)} \tag{21}$$

5.2. Experiment and result

Table 2 shows a data example of detection reports for threat assessment. As shown in Table 2, both RPS_1 and RPS_3 distribute a larger chance value to support the 1-type threat event (A), the 2-type threat event (A, B) and the 3-type threat event (A, C, B) compared to other events with the same type. Whereas, RPS_2 assigns a larger chance value to support the 1-type event (B), the 2-type event (B, A) and the 3-type event (B, A, C). RPS_1 and RPS_3 support each other and RPS_2 is relatively a "bad" report. Obviously, RPS_1 and RPS_3 have a larger reliability than RPS_2. The targets for different types of threat events in line with expectations should be (A), (A, B) and (A, C, B).

Based on Table 2, the proposed RAPJS is utilized to calculate the reliability values for three RPSs. Detailed steps are illustrated as below.

Step 1: Construct the distance matrix DM as follows:

$$DM = \begin{bmatrix} 0 & 0.2942 & 0.0732 \\ 0.2942 & 0 & 0.2601 \\ 0.0732 & 0.2601 & 0 \end{bmatrix}$$

Step 2: Obtain the average distance $\widetilde{D_{PJS}(RPS_i)}$:

$$\widetilde{D_{PJS}(RPS_1)} = 0.1837$$
$$\widetilde{D_{PJS}(RPS_2)} = 0.2771$$
$$\widetilde{D_{PJS}(RPS_3)} = 0.1607$$

Step 3: Calculate the support degree $Sup(RPS_i)$:

$$Sup(RPS_1) = 5.4438$$
$$Sup(RPS_2) = 3.6083$$
$$Sup(RPS_3) = 6.0003$$

Step 4: Compute the reliability degree $W(RPS_i)$:

$$W(RPS_1) = 0.3617$$
$$W(RPS_2) = 0.2397$$
$$W(RPS_3) = 0.3986$$

The reliability ranking for three RPSs is $W(RPS_3) > W(RPS_1) > W(RPS_2)$. Correspondingly, the fusion order is RPS_3, RPS_1 and RPS_2 successively.

Step 5: Obtain the fusion results by $RPS_3 \overline{\oplus} RRS_1 \overline{\oplus} RPS_2$:

The fusion results based on Eq. 15 are shown in Table 3:

Step 6: Calculate the relative threat degree:

The relative threat degrees for all types of threat events are computed based on Eq. 16, as below (see Table 4). :

Table 2
The threat assessment reports by three radars represented by RPS.

	(A)	(B)	(C)	(B,A)	(A,B)	(A,C)	(C,A,B)	(B,C,A)	(B,A,C)	(A,C,B)	(A,B,C)
RPS_1	0.2	0.08	0	0.05	0.12	0.03	0	0.05	0.1	0.25	0.12
RPS_2	0.07	0.13	0.02	0.2	0.07	0.1	0.08	0	0.2	0	0.13
RPS_3	0.14	0.09	0	0.08	0.12	0	0.05	0	0.1	0.3	0.12

Table 3
The fusion results of three RPSs.

	(A)	(B)	(C)	(A, B)	(B, A)	(A, C)	(C, A)	(A, B, C)	(A, C, B)	(B, A, C)	(C, A, B)
$\mathscr{M}^L(\cdot)$	0.349	0.196	0.007	0.198	0.071	0.039	0.004	0.029	0.072	0.024	0.012

Table 4
The relative threat degrees for threat events.

	(A)	(C)	(B)	(A, B)	(B, A)	(A, C)	(C, A)	(A, B, C)	(A, C, B)	(B, A, C)	(C, A, B)
$RTD(\cdot)$	0.632	0.013	0.355	0.635	0.227	0.126	0.012	0.211	0.526	0.175	0.088

Table 5
The combination results of RPSs in six cases.

Algorithm	Case 1 RPSDF	Case 2 RPSDF	Case 3 RPSDF	Case 4 RPSDF	Case 5 RPSDF	Case 6 RAPJS + RPSDF
(A)	0.349	0.349	0.349	0.349	0.349	0.349
(B)	0.196	0.196	0.196	0.196	0.196	0.196
(C)	0.007	0.007	0.007	0.007	0.007	0.007
(A, B)	0.19	0.19	0.097	0.097	0.198	0.198
(B, A)	0.078	0.078	0.172	0.172	0.071	0.071
(A, C)	0.04	0.04	0.041	0.041	0.039	0.039
(C, A)	0.003	0.003	0.002	0.002	0.004	0.004
(A, B, C)	0.031	0.031	0.043	0.043	0.029	0.029
(A, C, B)	0.065	0.065	0	0	0.072	0.072
(B, A, C)	0.026	0.026	0.066	0.066	0.024	0.024
(B, C, A)	0.013	0.013	0	0	0	0
(C, A, B)	0	0	0.027	0.027	0.012	0.012

Table 6
The relative threat degrees in six cases.

Algorithm	Case 1 RPSDF	Case 2 RPSDF	Case 3 RPSDF	Case 4 RPSDF	Case 5 RPSDF	Case 6 RAPJS + RPSDF
RTD (A)	0.632	0.632	0.632	0.632	0.632	0.632
RTD (B)	0.355	0.355	0.355	0.355	0.355	0.355
RTD (C)	0.013	0.013	0.013	0.013	0.013	0.013
RTD (A, B)	0.612	0.612	0.311	0.311	0.635	0.635
RTD (B, A)	0.25	0.25	0.551	0.551	0.227	0.227
RTD (A, C)	0.128	0.128	0.133	0.133	0.126	0.126
RTD (C, A)	0.01	0.01	0.005	0.005	0.012	0.012
RTD (A, B, C)	0.231	0.231	0.317	0.317	0.211	0.211
RTD (A, C, B)	0.481	0.481	0	0	0.526	0.526
RTD (B, A, C)	0.192	0.192	0.488	0.488	0.175	0.175
RTD (B, C, A)	0.096	0.096	0	0	0	0
RTD (C, A, B)	0	0	0.195	0.195	0.088	0.088

Table 7
The final threat assessments in six cases.

Algorithm	Case 1 RPSDF	Case 2 RPSDF	Case 3 RPSDF	Case 4 RPSDF	Case 5 RPSDF	Case 6 RAPJS + RPSDF
FTA_1	(A)	(A)	(A)	(A)	(A)	(A)
FTA_2	(A,B)	(A,B)	(B,A)	(B,A)	(A,B)	(A,B)
FTA_3	(A,C,B)	(A,C,B)	(B,A,C)	(B,A,C)	(A,C,B)	(A,C,B)

Step 7: Determine the final threat assessment:

Based on the maximum threat degree principle in Eq. 17, the final assessment results for each type of threat event are derived as follows:

$$FTA_1 = (A), \quad FTA_2 = (A, B), \quad FTA_3 = (A, C, B)$$

Therefore, the results show that if the enemy only dispatch one type of aircraft, the most likely alternative is (A). If the enemy dispatches two types of aircraft, the most likely formation and sequence is (A, B). If the enemy dispatches all types of aircraft, the most likely formation and sequence is (A, C, B).

5.3. Comparison and discussion

In order to show the advantage of the proposed RAPJS algorithm in determining the fusion order of RPSs, the other five cases with random fusion orders in RPSDF algorithm are compared, i.e., Case 1: $RPS_1 \overline{\oplus} RRS_3 \overline{\oplus} RPS_2$, Case 2: $RPS_1 \overline{\oplus} RRS_2 \overline{\oplus} RPS_3$, Case 3: $RPS_2 \overline{\oplus} RRS_1 \overline{\oplus} RPS_3$, Case 4: $RPS_2 \overline{\oplus} RRS_3 \overline{\oplus} RPS_1$, Case 5: $RPS_3 \overline{\oplus} RRS_2 \overline{\oplus} RPS_1$. By implementing the RPSDF algorithm, the combination results, as well as the relative threat degrees and the final threat assessment results under five cases are shown in Tables 5–7, respectively. In addition, the fusion order determined by the proposed RAPJS algorithm is named as Case 6: $RPS_3 \overline{\oplus} RRS_1 \overline{\oplus} RPS_2$, the relative results in Section 5.2 are also listed in Tables 5–7 for a clear comparison.

As shown in Table 7, in Case 1, Case 2, Case 5 and Case 6, the RPSDF algorithm can identify all different types of threat targets. Whereas, in Case 3 and Case 4, the RPSDF algorithm cannot handle the conflicting report (RPS_2) and comes to the wrong result that the 2-type threat event is (B,A) and the 3-type threat event is (B, A, C). Additionally, Case 6, where the fusion order is determined by the proposed RAPJS algorithm, has the highest accuracy values on threat events (A, B) and (A, C, B), as shown in Fig. 4. Consequently, the above analysis verify that the fusion order has a great impact on the performance of the RPSDF algorithm. Under the fusion order determined by the proposed RAPJS algorithm, the corresponding results are consistent with ideal targets and have the highest accuracy of evaluation. The reason is that the proposed RAPJS algorithm makes use of the function of Permutation Jensen–Shannon divergence to obtain the reliability information of RPSs. As a result, the performance in Case 6 shows the effectiveness and superiority of the proposed RAPJS algorithm.

In addition, two interesting findings can be found in Tables 6 and 7. One is that Case 1 and Case 2, Case 3 and Case 4, Case 5 and Case 6 have the same results. The other is that all these six cases identify A as the 1-type threat event with chance 0.632. Actually, these two situations are caused by the fusion mechanism of RPS itself (see Eq. (8)). LOS utilizes most of information in the first-fused RPS, but just keeps little information in the remaining RPSs. Therefore, the first-fused RPS plays a decisive role in fusion process. As for permutation events with single element like (A), they do not contain any order information. Hence different fusion orders have no effect on combination results for permutation events with single element.

6. Conclusion

This paper first proposes Permutation Jensen–Shannon (PJS) divergence for measuring the difference between two RPSs, and then put

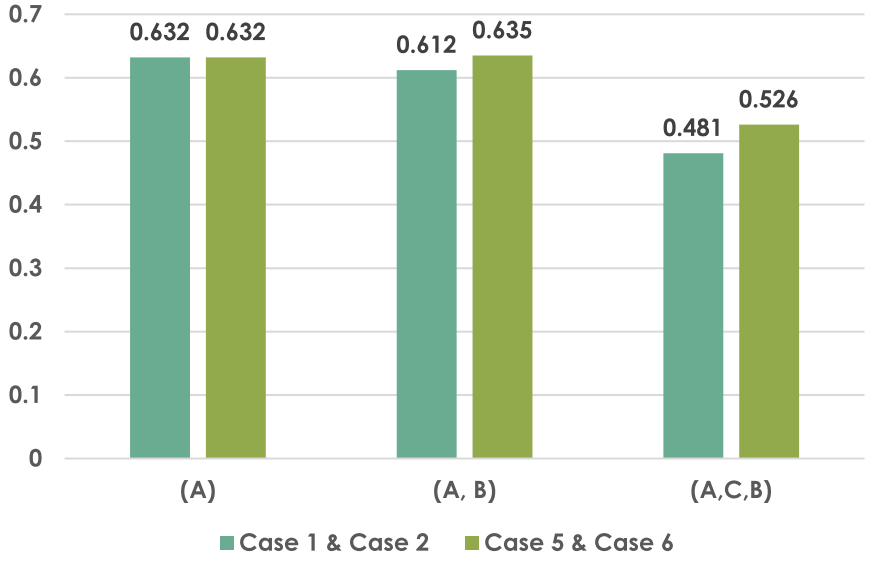

Fig. 4. PMFs on (A), (A, B) and (A, C, B) in Case 1, Case 2, Case 5 and Case 6.

forward a Reliability Assessment (RAPJS) algorithm for determining the fusion order of RPSs. As an efficient tool for measuring uncertainty with ordered information, RPS provides permutation orthogonal sum (POS) to fuse RPS sources. However, how to determine the fusion order in POS remains unsolved since different fusion orders will produce different fusion results. To address this problem, this paper has the following contributions:

- The divergence measure for RPS, named Permutation Jensen–Shannon (PJS) divergence, is being proposed in this paper. The presented PJS divergence is compatible with BJS divergence and the classic JS divergence. The proposed PJS degenerates into BJS when the order in permutation events is not considered, i.e., when PMF turns into mass function. The proposed PJS further collapses into JS when all of PMFs are assigned to single elements, i.e., when PMF turns into probability.
- Based on the proposed PJS divergence, a new reliability assessment algorithm (RAPJS) is further presented for determining the fusion order of RPSs. The RPS with a higher reliability is fused first. Experimental results in threat assessment show that the presented RAPJS can effectively determine the fusion order of RPSs, the corresponding fusion results are in agreement with expectations and have the highest recognition rate compared to results under other fusion orders.

Our proposed PJS divergence focuses on the discrepancy between two permutation mass function distributions, hence the difference between elements in permutation events is not considered, and this motivates future work. In addition, how to extend the proposed method for more real world applications is also worth exploring.

CRediT authorship contribution statement

Luyuan Chen: Conceptualization, Methodology, Writing – original draft, Writing – review & editing. **Yong Deng:** Validation, Resources, Writing – review & editing, Supervision, Funding acquisition. **Kang Hao Cheong:** Formal analysis, Validation, Writing – review & editing, Supervision.

Declaration of competing interest

The authors declare that they have no known competing financial interests or personal relationships that could have appeared to influence the work reported in this paper.

Data availability

No data was used for the research described in the article.

Acknowledgments

The authors greatly appreciate the editor's encouragement and the reviews' suggestions. The work is partially supported by National Natural Science Foundation of China (Grant No. 61973332), JSPS Invitational Fellowships for Research in Japan (Short-term).

References

Abualigah, L., Abd Elaziz, M., Sumari, P., Geem, Z.W., Gandomi, A.H., 2022. Reptile Search Algorithm (RSA): A nature-inspired meta-heuristic optimizer. Expert Syst. Appl. 191, 116158.

Abualigah, L., Diabat, A., Mirjalili, S., Abd Elaziz, M., Gandomi, A.H., 2021a. The arithmetic optimization algorithm. Comput. Methods Appl. Mech. Engrg. 376, 113609.

Abualigah, L., Yousri, D., Abd Elaziz, M., Ewees, A.A., Al-Qaness, M.A., Gandomi, A.H., 2021b. Aquila optimizer: a novel meta-heuristic optimization algorithm. Comput. Ind. Eng. 157, 107250.

Agushaka, J.O., Ezugwu, A.E., Abualigah, L., 2022a. Dwarf mongoose optimization algorithm. Comput. Methods Appl. Mech. Engrg. 391, 114570.

Agushaka, J.O., Ezugwu, A.E., Abualigah, L., 2022b. Gazelle optimization algorithm: a novel nature-inspired metaheuristic optimizer. Neural Comput. Appl. 1–33.

Atanassov, K.T., 1999. Intuitionistic fuzzy sets. In: Intuitionistic Fuzzy Sets. Springer, pp. 1–137.

Bordenave, C., Collins, B., 2019. Eigenvalues of random lifts and polynomials of random permutation matrices. Ann. of Math. 190 (3), 811–875.

Carabias-Orti, J.J., Rodríguez-Serrano, F.J., Vera-Candeas, P., Cañadas-Quesada, F.J., Ruiz-Reyes, N., 2013. Constrained non-negative sparse coding using learnt instrument templates for realtime music transcription. Eng. Appl. Artif. Intell. 26 (7), 1671–1680.

Chen, Z., Cai, R., 2022. A novel divergence measure of mass function for conflict management. Int. J. Intell. Syst. 37 (6), 3709–3735.

Chen, L., Deng, Y., 2022a. Entropy of random permutation set. Commun. Stat. Theory Methods Revised.

Chen, X., Deng, Y., 2022b. An evidential software risk evaluation model. Mathematics 10 (13), http://dx.doi.org/10.3390/math10132325.

Chen, L., Deng, Y., 2022c. An improved evidential Markov decision making model. Appl. Intell. 52 (7), 8008–8017.

Chen, L., Deng, Y., Cheong, K.H., 2021a. Probability transformation of mass function: A weighted network method based on the ordered visibility graph. Eng. Appl. Artif. Intell. 105, 104438.

Chen, X., Wang, T., Ying, R., Cao, Z., 2021b. A fault diagnosis method considering meteorological factors for transmission networks based on p systems. Entropy 23 (8), 1008.

Cui, H., Zhou, L., Li, Y., Kang, B., 2022. Belief entropy-of-entropy and its application in the cardiac interbeat interval time series analysis. Chaos Solitons Fractals 155, 111736.

Dempster, A.P., 1967. Upper and lower probabilities induced by a multivalued mapping. Ann. Math. Stat. 38 (2), 325–339.
Deng, Y., 2020. Uncertainty measure in evidence theory. Sci. China Inf. Sci. 63 (11), 1–19.
Deng, Y., 2022. Random permutation set. Int. J. Comput. Commun. Control 17 (1).
Deng, J., Deng, Y., 2022. Maximum entropy of random permutation set. Soft Comput. 1–11.
Deng, Z., Wang, J., 2021. A new evidential similarity measurement based on Tanimoto measure and its application in multi-sensor data fusion. Eng. Appl. Artif. Intell. 104, 104380.
Ezugwu, A.E., Agushaka, J.O., Abualigah, L., Mirjalili, S., Gandomi, A.H., 2022. Prairie dog optimization algorithm. Neural Comput. Appl. 1–49.
Fan, J., Wang, J., Wu, M., 2021. Extended two-dimensional belief function based on divergence measurement. J. Intell. Fuzzy Systems 40 (3), 4993–5000.
Gao, X., Pan, L., Deng, Y., 2022a. A generalized divergence of information volume and its applications. Eng. Appl. Artif. Intell. 108, 104584.
Gao, X., Su, X., Qian, H., Pan, X., 2022b. Dependence assessment in human reliability analysis under uncertain and dynamic situations. Nuclear Eng. Technol. 54 (3), 948–958.
Gao, R., Zhang, J., Xiao, W., Li, Y., 2019. Kullback–Leibler divergence based probabilistic approach for device-free localization using channel state information. Sensors 19 (21), 4783.
Jiao, Z., Ran, L., Zhang, Y., Li, Z., Zhang, W., 2018. Data-driven approaches to integrated closed-loop sustainable supply chain design under multi-uncertainties. J. Clean. Prod. 185, 105–127.
Joshi, R., Kumar, S., 2019a. A dissimilarity measure based on Jensen Shannon divergence measure. Int. J. Gen. Syst. 48 (3), 280–301.
Joshi, R., Kumar, S., 2019b. Exponential jensen intuitionistic fuzzy divergence measure with applications in medical investigation and pattern recognition. Soft Comput. 23 (18), 8995–9008.
Joshi, R., Kumar, S., 2019c. Jensen-Tsalli's intuitionistic fuzzy divergence measure and its applications in medical analysis and pattern recognition. Int. J. Uncertain. Fuzziness Knowl.-Based Syst. 27 (01), 145–169.
Kharazmi, O., Balakrishnan, N., 2021. Jensen-information generating function and its connections to some well-known information measures. Statist. Probab. Lett. 170, 108995.
Kharazmi, O., Balakrishnan, N., Jamali, H., 2022. Cumulative Residual q-Fisher Information and Jensen-Cumulative Residual χ 2 Divergence Measures. Entropy 24 (3), 341.
Lai, J.W., Chang, J., Ang, L.K., Cheong, K.H., 2020. Multi-level information fusion to alleviate network congestion. Inf. Fusion 63, 248–255.
Lee, P., 1980. Probability theory. Bull. Lond. Math. Soc. 12 (4), 318–319.
Li, Y., Qin, K., He, X., 2014. Dissimilarity functions and divergence measures between fuzzy sets. Inform. Sci. 288, 15–26.
Lin, J., 1991. Divergence measures based on the Shannon entropy. IEEE Trans. Inform. Theory 37 (1), 145–151.
Liu, Z., Zhang, X., Niu, J., Dezert, J., 2020. Combination of classifiers with different frames of discernment based on belief functions. IEEE Trans. Fuzzy Syst. 29 (7), 1764–1774.
Mishra, A.R., Rani, P., Mardani, A., Kumari, R., Zavadskas, E.K., Kumar Sharma, D., 2020a. An extended Shapley TODIM approach using novel exponential fuzzy divergence measures for multi-criteria service quality in vehicle insurance firms. Symmetry 12 (9), 1452.
Mishra, A.R., Rani, P., Pardasani, K.R., Mardani, A., Stević, Ž., Pamučar, D., 2020b. A novel entropy and divergence measures with multi-criteria service quality assessment using interval-valued intuitionistic fuzzy TODIM method. Soft Comput. 24 (15), 11641–11661.
Moreno, P., Ho, P., Vasconcelos, N., 2003. A Kullback-Leibler divergence based kernel for SVM classification in multimedia applications. Adv. Neural Inf. Process. Syst. 16.
Oyelade, O.N., Ezugwu, A.E.-S., Mohamed, T.I., Abualigah, L., 2022. Ebola optimization search algorithm: A new nature-inspired metaheuristic optimization algorithm. IEEE Access 10, 16150–16177.
Pan, L., Gao, X., Deng, Y., Cheong, K.H., 2022. Enhanced mass Jensen–Shannon divergence for information fusion. Expert Syst. Appl. 209, 118065.
Pan, Y., Zhang, L., Wu, X., Skibniewski, M.J., 2020. Multi-classifier information fusion in risk analysis. Inf. Fusion 60, 121–136.
Qiang, C., Deng, Y., Cheong, K.H., 2022. Information fractal dimension of mass function. Fractals 30 (6), 2250110.
Rani, P., Mishra, A.R., Pardasani, K.R., Mardani, A., Liao, H., Streimikiene, D., 2019. A novel VIKOR approach based on entropy and divergence measures of Pythagorean fuzzy sets to evaluate renewable energy technologies in India. J. Clean. Prod. 238, 117936.
Shafer, G., 1976. A Mathematical Theory of Evidence, Vol. 1. Princeton university press Princeton.
Shang, M., Yuan, Y., Luo, X., Zhou, M., 2021. An α-β-divergence-generalized recommender for highly accurate predictions of missing user preferences. IEEE Trans. Cybern. http://dx.doi.org/10.1109/TCYB.2020.3026425.
Song, Y., Fu, Q., Wang, Y.-F., Wang, X., 2019. Divergence-based cross entropy and uncertainty measures of Atanassov's intuitionistic fuzzy sets with their application in decision making. Appl. Soft Comput. 84, 105703.
Song, Y., Wang, X., Zhu, J., Lei, L., 2018. Sensor dynamic reliability evaluation based on evidence theory and intuitionistic fuzzy sets. Appl. Intell. 48 (11), 3950–3962.
Song, X., Xiao, F., 2022. Combining time-series evidence: A complex network model based on a visibility graph and belief entropy. Appl. Intell. 1–10.
Tang, M., Liao, H., Herrera-Viedma, E., Chen, C.P., Pedrycz, W., 2020. A dynamic adaptive subgroup-to-subgroup compatibility-based conflict detection and resolution model for multicriteria large-scale group decision making. IEEE Trans. Cybern. 51 (10), 4784–4795.
Wang, H., Deng, X., Jiang, W., Geng, J., 2021. A new belief divergence measure for Dempster–Shafer theory based on belief and plausibility function and its application in multi-source data fusion. Eng. Appl. Artif. Intell. 97, 104030.
Wen, T., Cheong, K.H., 2021. The fractal dimension of complex networks: A review. Inf. Fusion 73, 87–102.
Wen, Z., Liu, Z., Zhang, S., Pan, Q., 2021. Rotation awareness based self-supervised learning for sar target recognition with limited training samples. IEEE Trans. Image Process. 30, 7266–7279.
Wu, M.-Q., Chen, T.-Y., Fan, J.-P., 2019. Divergence measure of T-spherical fuzzy sets and its applications in pattern recognition. IEEE Access 8, 10208–10221.
Wu, Y., Ding, H., Gong, M., Qin, A.K., Ma, W., Miao, Q., Tan, K.C., 2022a. Evolutionary multiform optimization with two-stage bidirectional knowledge transfer strategy for point cloud registration. IEEE Trans. Evol. Comput. 1. http://dx.doi.org/10.1109/TEVC.2022.3215743.
Wu, M., Hou, X., Fan, J., 2022b. Improvement of cross-efficiency based on TODIM method. Soft Comput. 26 (17), 8427–8439.
Wu, Y., Li, J., Yuan, Y., Qin, A., Miao, Q.-G., Gong, M.-G., 2021. Commonality autoencoder: Learning common features for change detection from heterogeneous images. IEEE Trans. Neural Netw. Learn. Syst. http://dx.doi.org/10.1109/TNNLS.2021.3056238.
Wu, Y., Liu, Y., Gong, M., Gong, P., Li, H., Tang, Z., Miao, Q., Ma, W., 2022c. Multi-view point cloud registration based on evolutionary multitasking with bi-channel knowledge sharing mechanism. IEEE Trans. Emerg. Top. Comput. Intell. http://dx.doi.org/10.1109/TETCI.2022.3205384.
Wu, Y., Zhang, Y., Fan, X., Gong, M., Miao, Q., Ma, W., 2022d. INENet: Inliers estimation network with similarity learning for partial overlapping registration. IEEE Trans. Circuits Syst. Video Technol. 1. http://dx.doi.org/10.1109/TCSVT.2022.3213592.
Xiao, F., 2019. Multi-sensor data fusion based on the belief divergence measure of evidences and the belief entropy. Inf. Fusion 46, 23–32.
Xiao, F., 2020. A new divergence measure for belief functions in D–S evidence theory for multisensor data fusion. Inform. Sci. 514, 462–483.
Xiao, F., 2022. CaFtR: A fuzzy complex event processing method. Int. J. Fuzzy Syst. 24 (2), 1098–1111.
Xiao, F., Pedrycz, W., 2022. Negation of the quantum mass function for multisource quantum information fusion with its application to pattern classification. IEEE Trans. Pattern Anal. Mach. Intell..
Xu, S., Hou, Y., Deng, X., Chen, P., Ouyang, K., Zhang, Y., 2021. A novel divergence measure in Dempster–Shafer evidence theory based on pignistic probability transform and its application in multi-sensor data fusion. Int. J. Distrib. Sens. Netw. 17 (7), 15501477211031473.
Yang, Y., Han, D., 2016. A new distance-based total uncertainty measure in the theory of belief functions. Knowl.-Based Syst. 94, 114–123.
Yuan, Y., He, Q., Luo, X., Shang, M., 2020. A multilayered-and-randomized latent factor model for high-dimensional and sparse matrices. IEEE Trans. Big Data http://dx.doi.org/10.1109/TBDATA.2020.2988778.
Yuan, Y., Luo, X., Shang, M., Wang, Z., 2022. A Kalman-filter-incorporated latent factor analysis model for temporally dynamic sparse data. IEEE Trans. Cybern. http://dx.doi.org/10.1109/TCYB.2022.3185117.
Zadeh, L.A., 1996. Fuzzy sets. In: Fuzzy Sets, Fuzzy Logic, and Fuzzy Systems: Selected Papers by Lotfi a Zadeh. World Scientific, pp. 394–432.
Zhang, H., Deng, Y., 2021. Entropy measure for orderable sets. Inform. Sci. 561, 141–151.
Zhang, Y., Hu, S., Zhou, W., 2020. Multiple attribute group decision making using J-divergence and evidential reasoning theory under intuitionistic fuzzy environment. Neural Comput. Appl. 32 (10), 6311–6326.
Zhang, Z., Wang, H., Geng, J., Jiang, W., Deng, X., Miao, W., 2022. An information fusion method based on deep learning and fuzzy discount-weighting for target intention recognition. Eng. Appl. Artif. Intell. 109, 104610.
Zhao, K., Li, L., Chen, Z., Sun, R., Yuan, G., Li, J., 2022. A survey: Optimization and applications of evidence fusion algorithm based on Dempster-Shafer theory. Appl. Soft Comput. 109075.
Zhao, K., Sun, R., Li, L., Hou, M., Yuan, G., Sun, R., 2021. An optimal evidential data fusion algorithm based on the new divergence measure of basic probability assignment. Soft Comput. 25 (17), 11449–11457.
Zhou, Q., Deng, Y., Pedrycz, W., et al., 2022. Information dimension of galton board. FRACTALS (Fractals) 30 (04), 1–11.